Hydraulic Performance Curves for Highway Culverts

Randall J. Charbeneau, M.ASCE[1]; Andrew D. Henderson[2]; and Lee C. Sherman, M.ASCE[3]

Abstract: This paper presents a versatile two-parameter model describing the hydraulic performance of highway culverts operating under inlet control for both unsubmerged and submerged conditions. Applications show that the model can accurately represent the Federal Highway Administration (FHwA) performance curves (which use four parameters) for a range of culvert types and materials. Laboratory data from an investigation of the hydraulic performance of single- and multiple-barrel low-headwater box culverts are also used, and the resulting model predicts a smaller culvert size as compared with the FHwA equations for a given design discharge. Design recommendations are presented for low-headwater box culverts.

DOI: 10.1061/(ASCE)0733-9429(2006)132:5(474)

CE Database subject headings: Culverts; Performance characteristics; Coefficients; Critical flow; Highways.

Introduction

The performance curve for a culvert specifies the relationship between the headwater and culvert barrel discharge. In the development of performance curves, data from unsubmerged and submerged inlet control conditions are often evaluated separately. This results in unsubmerged and submerged performance curves that may or may not overlap, and identification of the transition between these conditions is uncertain. In this paper, a simple two-parameter model for the culvert performance curve is developed. The resulting model has a smooth, well-defined transition between the unsubmerged and submerged hydraulic conditions. Application to the Federal Highway Administration (FHwA) performance curves shows that the model is versatile, providing a very good representation for a range of culvert types and materials. The performance of low-headwater multiple-barrel box culverts is discussed in more detail, including results from an experimental investigation of the hydraulic effects of an upstream channel expansion leading to multiple-barrel box culverts.

Culvert Hydraulics

One focus of this research is the performance curve of a box culvert operating under inlet control. Inlet control occurs when the culvert barrel is capable of conveying more flow than the inlet will accept. The control section of a culvert operating under inlet control is located just inside the entrance. Critical depth occurs at or near this location, and the flow regime immediately downstream is supercritical (Normann et al. 1985). Only the headwater and the inlet configuration affect the culvert performance. Important factors include headwater depth, inlet area, barrel shape, and inlet edge configuration.

Under inlet control, the culvert performance may be described as either unsubmerged or submerged, depending on the headwater depth. The transition between these conditions is not well defined. If the entrance is unsubmerged, then its culvert hydraulic performance is similar to (broad-crested) weir flow (Normann et al. 1985; ASCE 1992). Based on the assumptions that critical flow is established within the culvert barrel near the entrance and that head losses between the headwater and control section are negligible, the energy equation gives

$$HW = E_c = y_c + (Q/C_b B y_c)^2/2g \tag{1}$$

In Eq. (1), HW=upstream headwater (specific energy) measured from the culvert invert elevation; E_c=critical specific energy at the control section within the culvert entrance; y_c=critical depth at the control section; Q=barrel discharge; C_b=coefficient expressing effective width contraction associated with the culvert entrance edge conditions; B=culvert span (width); and g=gravitational constant. For critical flow in a rectangular box culvert, $y_c = 2/3E_c = 2/3HW$, which allows Eq. (1) to be written in the following form as a performance equation:

$$\frac{HW}{D} = \frac{3}{2}\left(\frac{1}{C_b}\right)^{2/3}\left(\frac{Q}{A\sqrt{gD}}\right)^{2/3} \tag{2}$$

In Eq. (2), D=culvert rise (height); and A=full culvert cross-section area ($A=BD$ for a box culvert).

When the culvert entrance is submerged, then the culvert performance may be described either as an orifice (Normann et al. 1985; ASCE 1992) or as a sluice gate (Henderson 1966). Consider the configuration shown in Fig. 1. With HW representing the headwater specific energy, application of the energy equation gives

$$HW = \frac{v_{en}^2}{2g} + C_c D \tag{3}$$

In Eq. (3), v_{en}=velocity within the culvert entrance; and C_c=contraction coefficient associated with flow passing the cul-

[1]Professor of Civil Engineering, Center for Research in Water Resources, The Univ. of Texas, Austin, TX 78712.

[2]Graduate Student, Dept. of Civil and Environmental Engineering, Univ. of Michigan, Ann Arbor, MI 48109.

[3]Staff Engineer, CDM, 5400 Glenwood Ave., Ste. 300, Raleigh, NC 27612.

Note. Discussion open until October 1, 2006. Separate discussions must be submitted for individual papers. To extend the closing date by one month, a written request must be filed with the ASCE Managing Editor. The manuscript for this paper was submitted for review and possible publication on February 25, 2003; approved on June 23, 2005. This paper is part of the ***Journal of Hydraulic Engineering***, Vol. 132, No. 5, May 1, 2006. ©ASCE, ISSN 0733-9429/2006/5-474–481/$25.00.

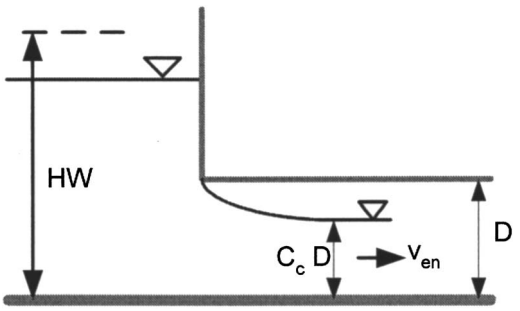

Fig. 1. Culvert entrance acting as a submerged sluice gate, with soffit contraction coefficient C_c

vert soffit. Energy losses between the upstream (headwater) station and the culvert entrance have again been neglected. Such losses are included within the coefficients C_b and C_c. Using Eq. (3), the culvert discharge is calculated from

$$Q = (C_b B)(C_c D)v_{en} = C_b C_c A\sqrt{2g(HW - C_c D)} \tag{4}$$

Eq. (4) may be written as a performance equation as follows:

$$\frac{HW}{D} = \frac{1}{2(C_b C_c)^2}\left(\frac{Q}{A\sqrt{gD}}\right)^2 + C_c \tag{5}$$

Eqs. (2) and (5) represent dimensionless performance curves for culverts operating under inlet control for unsubmerged and submerged inlet conditions. To find the transition between unsubmerged and submerged conditions, Eqs. (2) and (5) may be combined, eliminating the discharge term and resulting in the following:

$$\left(\frac{HW}{C_c D}\right)^3 - \frac{27}{4}\left(\frac{HW}{C_c D}\right) + \frac{27}{4} = 0 \tag{6}$$

The roots of this cubic equation are 3/2 (which is a double root) and −3. Only the positive root(s) are physically possible. Thus, the model equation transition between the unsubmerged and submerged conditions occurs at

$$\frac{HW}{D} = \frac{3}{2}C_c \tag{7}$$

$$\frac{Q}{A\sqrt{gD}} = C_b C_c^{3/2} \tag{8}$$

Furthermore, the slope at this point of contact between the two model equations is the same for both curves and is equal to

$$\frac{d\left(\frac{HW}{D}\right)}{d\left(\frac{Q}{A\sqrt{gD}}\right)} = \frac{1}{C_d\sqrt{C_c}} \tag{9}$$

Thus, the curves not only cross at this point, they become tangent to each other. This results in a smooth and well-defined transition between model equations for the unsubmerged and submerged conditions.

Previous Investigations of Culvert Hydraulics

Investigations of culvert hydraulics have generally concerned culvert performance under a wide range of headwater and tailwater elevations for different culvert shapes, materials, and inlet configurations (Yarnell et al. 1926; Mavis 1943; Metzler and Rouse 1959; Chow 1959; Henderson 1966). Under the sponsorship of the Bureau of Public Roads (now the Federal Highway Administration, FHwA), the National Bureau of Standards (now the National Institute of Science and Technology, NIST) conducted an extensive series of experiments to better define the performance of culverts. This research was performed during the 1950s and 1960s and forms the basis for many culvert design procedures and computer programs. French (1955) outlines the general scope of the investigations and presents hydraulic characteristics for circular and pipe-arch barrel shapes. French (1966) considers box culverts with nonenlarged (not tapered) inlets and constant barrel size operating under conditions of entrance control, with the objective of identifying the hydraulic performance of different leading edge geometries.

Based on the studies performed by the NIST, the FHwA developed a series of performance curves and nomographs for calculation of culvert performance under both inlet and outlet control for many commonly used entrance configurations and culvert materials (Herr and Bossy 1965; Normann et al. 1985). For unsubmerged inlet conditions, FHwA presents two relationships for the performance curve (Normann et al. 1985) that may be written in dimensionless form as follows:

$$\frac{HW}{D} = \frac{E_c}{D} + Kg^{M/2}\left[\frac{Q}{A\sqrt{gD}}\right]^M - 0.5S \tag{10}$$

$$\frac{HW}{D} = Kg^{M/2}\left[\frac{Q}{A\sqrt{gD}}\right]^M \tag{11}$$

In Eqs. (10) and (11), E_c=specific energy (head) at critical depth; Q=culvert barrel discharge; A=full cross-sectional area of the culvert barrel; S=culvert barrel slope; and K and M=model coefficients that depend on the culvert configuration. For submerged inlet conditions, the data from experiments performed by NIST for the FHwA have been fit to an equation of the form

$$\frac{HW}{D} = cg\left[\frac{Q}{A\sqrt{gD}}\right]^2 + Y - 0.5S \tag{12}$$

In Eq. (12), c and Y=coefficients that depend on the culvert shape, material, and inlet configuration.

Other types of hydraulic structures perform similarly to culverts, and investigations of their behavior provide insight on culvert performance. With critical flow established within the culvert entrance for unsubmerged flow conditions, the culvert acts to choke the channel (Henderson 1966). Investigations of channel contractions and choked flows (Wu and Molinas 2001) may be used to identify the factors that determine the magnitude of the coefficient C_b in Eq. (2). Wu and Molinas (2001) show how the discharge coefficient for a choked channel contraction depends on the opening ratio (ratio of culvert span to channel width), inlet (wingwall) angle, entrance shape, and contraction length. Their discharge equation [analogous to Eq. (2)] is written in terms of upstream water depth rather than headwater specific energy, so their discharge coefficient also depends on the upstream Froude number [see Eq. (21)]. Results from the earlier theoretical and

J. Hydraul. Eng. 2006.132:474-481.

laboratory investigations of Hager and Dupraz (1985) are used to assess the effects of the inlet angle on the (sidewall) contraction coefficient.

When the culvert entrance becomes submerged, the culvert performs like a sluice gate, or with curved soffit, like a radial gate. Basic information on the performance of sluice and radial gates is provided by Henderson (1966) and Bos (1989). Montes (1997) uses inviscid flow theory, numerical, and analytical methods to evaluate flow behavior for a planar sluice gate. Montes suggests that the larger contraction coefficients as compared to theory predictions are attributed to energy losses. Clemmens et al. (2003) consider calibration of radial gates for both free-flowing and (tailwater) submerged conditions, including the variation of the contraction coefficient with gate angle. Tailwater submerged conditions for a gate, as applied to culvert performance, would correspond to culverts operating under outlet control.

Application with FHwA Performance Equations

The FHwA performance equations, Eqs. (10)–(12), remain the most widely used for culvert design through hand calculation, nomographs (Herr and Bossy 1965; Normann et al. 1985), or computer models such as HEC-RAS (Brunner 2002). The model equations use four parameters (K, M, c, and Y). Estimation of flow conditions near the transition between unsubmerged and submerged performance curves usually requires manual or other adjustment [Normann et al. (1985); see also the Appendix]. The parameters for different culvert shapes, materials, and configurations are provided in Normann et al. (1985) [also see Sturm (2001)].

Fig. 2(a) shows the FHwA performance curve for a box culvert with 90° and 15° wingwall flares (Chart No. 8, Nomograph Scale 2) along with the fitted model using Eqs. (2) and (5), which is designated as the UT-CRWR curve. Model calibration is performed using the least-squares method with data from the FHwA curves [Eqs. (10) and (12) for this case] with discharge variables ranging from 0 to 1.2 in 0.025 increments (a total of 49 points) and model transition determined by the conditions specified in Eq. (8). The resulting coefficients are C_b=0.815 and C_c=0.754, and the transition between the unsubmerged and submerged conditions occurs at HW/D=1.132, $Q/[A(gD)^{0.5}]$=0.534. The standard error (SE) for this model fit is 0.0152 (error in fitting HW/D values).

The model presented in Eqs. (2) and (5) is robust, meaning that its range of application extends beyond the assumptions used in its derivation (C_b and C_c correspond to side and soffit contraction coefficients). Fig. 2(b) shows the FHwA model and the UT-CRWR model fit for a circular concrete culvert with "groove end with headwall" (Chart No. 1, Nomograph Scale 2). Again, the fit is excellent, though here, the coefficients C_b and C_c are viewed as fitting parameters. Fig. 2(c) shows the model results for a rectangular culvert with "tapered inlet throat" (FHwA Chart 57, Nomograph Scale 1). For this case, the FHwA model uses Eqs. (11) and (12). The fitted-model data for FHwA Charts 1, 8, and 57 are presented in Table 1. The cases with larger SE correspond to cases with larger divergence between the FHwA equations for the unsubmerged and submerged conditions. Overall, the model Eqs. (2) and (5) are found to be versatile for fitting performance curves for a wide range of culvert types and shapes, including rectangular, circular, elliptical, and pipe arch.

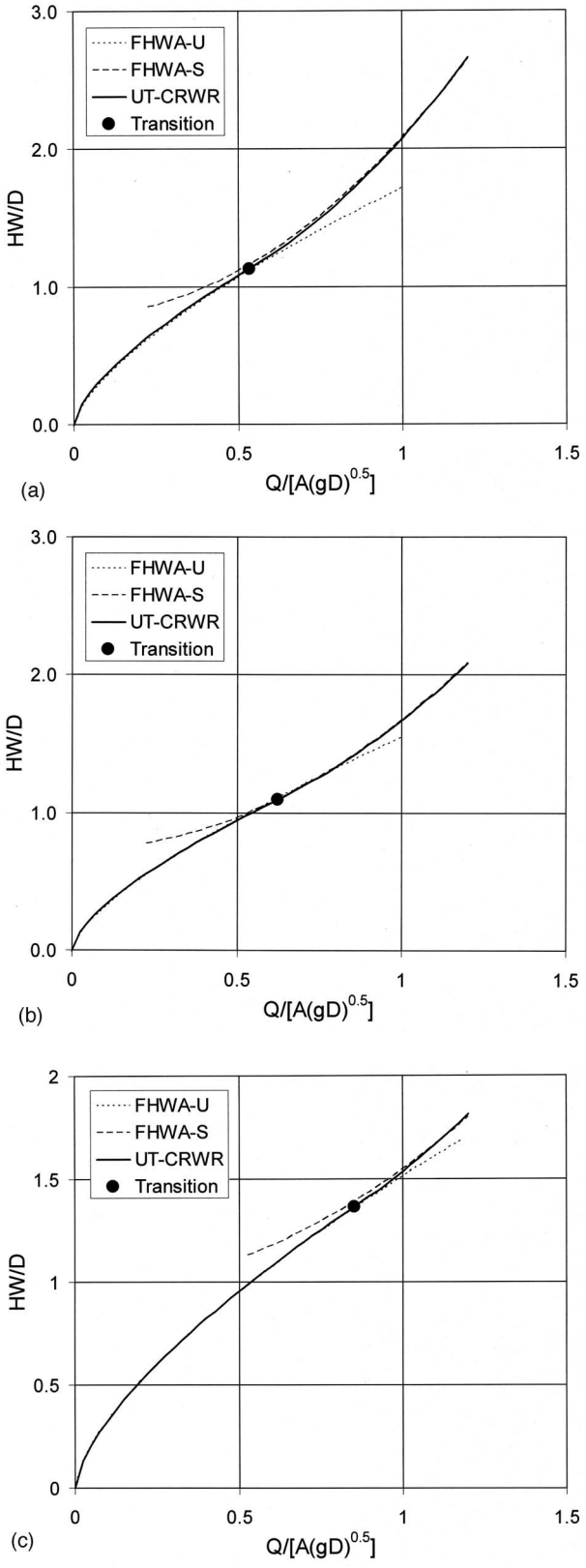

Fig. 2. Fitting of FHwA performance curves: (a) box culvert with 90° and 15° wingwall flares; (b) circular concrete culvert with groove end with headwall; and (c) rectangular culvert with tapered inlet throat

J. Hydraul. Eng. 2006.132:474-481.

Table 1. Constants for UT-CRWR Performance Curve

Culvert type	Description	C_b	C_c	SE
Circular concrete	Square edge with headwall	0.944	0.662	0.0108
Circular concrete	Groove end with headwall	1.000	0.729	0.0051
Circular concrete	Groove end projecting	0.998	0.712	0.0138
Rectangular box	30–75° wingwall flares	0.854	0.752	0.0371
Rectangular box	90 and 15° wingwall flares	0.815	0.754	0.0152
Rectangular box	0° wingwall flares	0.792	0.749	0.0272
Rectangular	Tapered inlet throat	0.982	0.910	0.0072

Application with Laboratory Data

A physical modeling research program was undertaken to investigate hydraulics of channel expansions leading to low-headwater box culverts, with emphasis on multiple-barrel culvert systems. Low-headwater box culverts are used along highways in areas with low topographic relief where highway rise associated with roadway embankments over drainage channels is kept small, and the corresponding upstream headwater must also remain low to prevent water overtopping the roadway under design-flow conditions. For such conditions, the design headwater depth may be limited to the culvert rise, and the velocity head contribution to the headwater specific energy may be significant.

The research program experiments included single- and multiple-barrel box culverts. For the primary set of experiments, the prototype model is based on a six-barrel box culvert with each culvert barrel having a span $B=3.05$ m (10 ft) and rise $D=1.83$ m (6 ft). A 1:10 scale ratio between the model and prototype sizes was selected for the laboratory experiments.

The physical model was developed to investigate the hydraulics of channel expansions located upstream of low-headwater box culvert systems. The primary features are an upstream trapezoidal channel and a downstream channel expansion section that contains the culvert model system. Fig. 3 outlines the layout of the physical model. The channel is divided into two primary sections. The upstream channel section leads from the headbox shown to the left of the figure downstream to the channel expansion. The upstream section cross section has a bottom width of 0.6 m and a side slope $2.5(H):1(V)$. The length of the upstream section is 9.8 m and channel slope in this section is 0.00038. The channel expansion section also has a trapezoidal cross section with bottom width 3.4 m and side slope $2(H):1(V)$. The total length of this section along the channel axis is 8.3 m. The longitudinal slope of this section was determined to be 0.0025. For most of the experiments the tailgate was set to allow no backwater effects, because the prototype downstream channel is wide and relatively free of flow obstructions. Fig. 4(a) shows the experiment six-barrel culvert system model, including the upstream

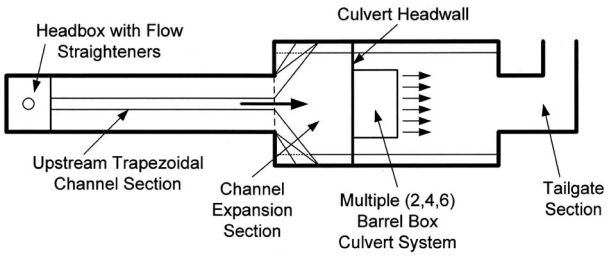

Fig. 3. Schematic plan view of physical model

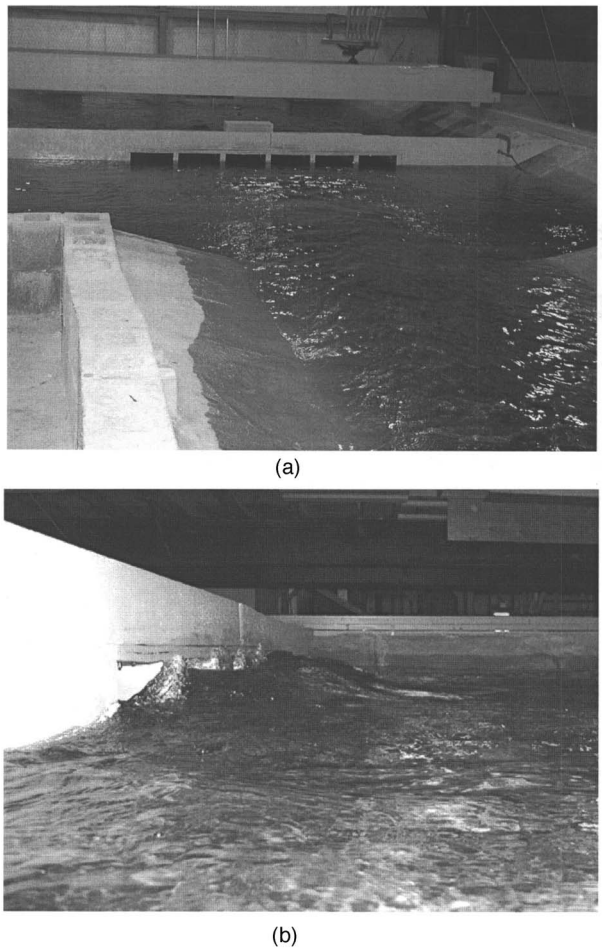

Fig. 4. (a) Physical model of six-barrel box culvert system with upstream trapezoidal channel and (b) water profile showing standing wave development near culvert entrance with rapid approach velocity

trapezoidal channel. Fig. 4(b) shows a side view of the water surface profile that develops immediately in front of the culvert entrance under conditions with a rapid approach velocity.

The data collected in this investigation include the channel discharge, water depth, water velocity, depth averaged water velocity, and specific energy. Additional details on the experimental program are provided in Charbeneau et al. (2002).

Experiments were performed with various combinations of two, four, and six barrels open and for different flow rates. Other experiments were performed in an outdoor channel with a single-barrel culvert, also operating under inlet control. Two different barrel spans were evaluated in the single-barrel outdoor channel. For each set of experiments, the total discharge was measured as well as the depth and velocity upstream of each barrel.

When fitting the measured data and the performance-curve model equations to estimate the unknown coefficients C_b and C_c, one difficulty that arises with the multiple-barrel culverts is that, while the total channel discharge is known, the discharge through each barrel is not. Measurements show that the headwater is lower for the outer barrels than for those located closer to the channel centerline, and it is clear that the discharge is not the same for each barrel. In order to utilize all of the data, the following approach is taken. Using the measured headwater for each barrel, the performance equations are used to predict the barrel

J. Hydraul. Eng. 2006.132:474-481.

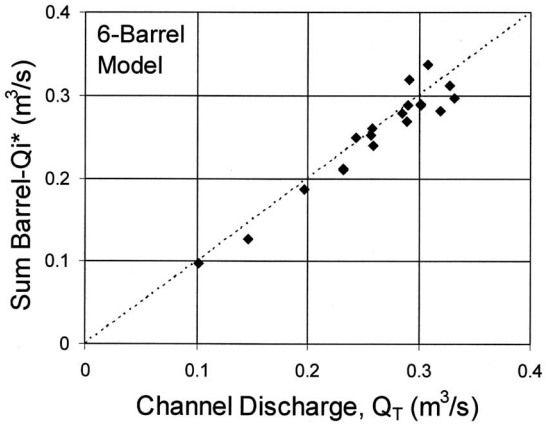

Fig. 5. Comparison of measured channel discharge with calculated cumulative barrel discharge (without correction)

discharge. The individual barrel discharge values are then corrected using the following equation:

$$Q_i = Q_i^* \times \frac{Q_T}{\sum_i Q_i^*} \tag{13}$$

In Eq. (13), Q_i=corrected barrel discharge; Q_i^*=calculated barrel discharge using the measured barrel headwater and the performance equation; and Q_T=measured channel discharge. The data correction specified by Eq. (13) gives a set of data that is consistent with the individual barrel headwater measurements and the measured total channel discharge. Moreover, the impact of this data correction on the overall data analysis is not significant. Fig. 5 compares the measured channel discharge with the cumulative barrel discharge without correction, showing that the effects of the discharge correction are not significant.

Fig. 6(a) shows the experimental data (N=174) for the one-, two-, four-, and six-barrel culvert systems. The coefficients in the model equations are fit to the data set using the method of least squares. For each measured data value $(HW/D)_d$, the model equations are used to calculated a model value $(Q/[A(gD)^{0.5}])_m$. The model discharge value is then compared with the measured data value, and the standard error is calculated from

$$\text{SE} = \sqrt{\frac{1}{N}\sum_{i=1}^{N}\left\{\left(\frac{Q}{A\sqrt{gD}}\right)_{mi} - \left(\frac{Q}{A\sqrt{gD}}\right)_{di}\right\}^2} \tag{14}$$

The resulting parameter values are C_b=1.098 and C_c=0.574. The corresponding standard error is SE=0.0369.

One of the difficulties with the initial model fit is the estimated value of the C_b coefficient. The physical interpretation is that C_b expresses a contraction coefficient that reflects the inward (centerline) momentum associated with flow around the vertical edges of the box culvert. As such, for a box culvert it should have a maximum value of 1.0 for effectively rounded edges. However, C_b appears in both the unsubmerged and submerged performance curves, as well as in the discharge equation specifying the transition between these flow conditions. The resulting parameter estimate is based on data from both the unsubmerged and submerged flow conditions, as well as the model constraining conditions which result in a smooth transition. The overall data set results in a value of C_b that is larger than expected. In addition, some of the data shown in Fig. 6(a) are not consistent with the model assumption of inlet control. With multiple barrels open (four or six), the

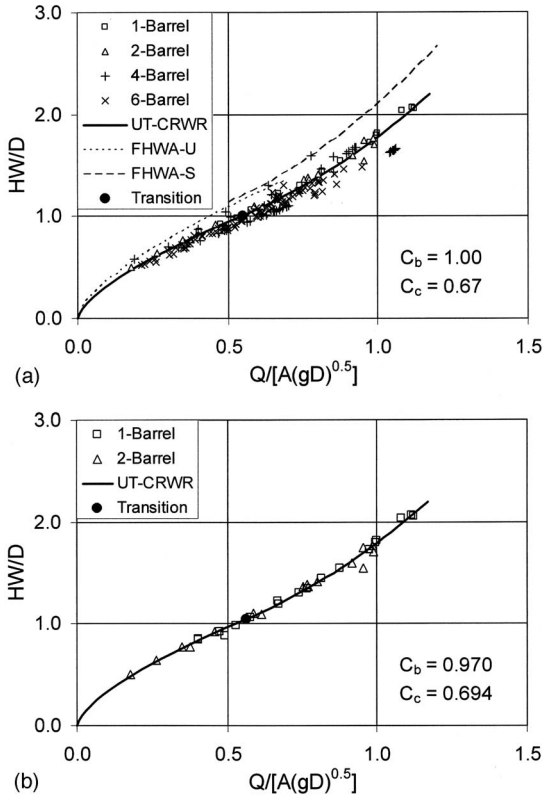

Fig. 6. (a) Multiple-barrel box culvert data and performance curve (labeled UT-CRWR), where curve labeled "FHwA-U" is Eq. (10) and curve "FHwA-S" is Eq. (12) and (b) single and two-barrel culvert data with fitted performance curve

headwater for some of the data corresponds to supercritical flow ($F>1$). Supercritical flow is generally not consistent with inlet control, because the headwater is not free to adjust to the inlet configuration for a given barrel discharge. However, as discussed in the Appendix, the data presented in Fig. 6(a) appears to be consistent with the model Eqs. (2) and (5) in terms of headwater and discharge values. Fig. 6(b) shows only a subset of the data from Fig. 6(a) for single- and two-barrel culverts. All data in Fig. 6(b) correspond to subcritical flow. The resulting model coefficients are C_b=0.970 and C_c=0.694, with SE=0.020 based on the N=35 data points. The model curve shows an excellent fit to the data, especially in the unsubmerged flow region.

In order to reflect the physical interpretation of C_b, the minimum standard error was again evaluated for the entire data set with a constraint that C_b=1.0. With this constraint, the minimum standard error was found to be SE=0.0484, with corresponding parameter values C_b=1.0, C_c=0.670. This is an increase in standard error of almost 30% as compared with the unconstrained case. The resulting performance curve is shown in Fig. 6(a), along with the FHwA performance curves predicted from Eqs. (10) and (12). The significant difference between the FHwA curves and the measurements is evident.

Comparison with Literature Contraction Coefficient Values

Metzler and Rouse (1959) suggest a performance equation for unsubmerged inlet conditions that has a form similar to Eq. (2).

J. Hydraul. Eng. 2006.132:474-481.

While they do not give specific values for coefficients, interpretation of the data presented in their Fig. 15 suggests that $C_b=0.85$ for both sharp and rounded inlet edges. Henderson (1966) also presents Eq. (2) as a performance equation for unsubmerged inlet conditions and states that, if the vertical edges are rounded to a radius of $0.1B$ or more, there is no side contraction and $C_b=1$. If the vertical edges are left square, Henderson gives $C_b=0.9$. French (1966) presents experimental data supporting Eq. (2). For square and rectangular box culverts with square edges, French finds contraction coefficients, C_b, that range from 0.87 to 0.91, with an average value near 0.88, a value close to that suggested by Henderson. Data from French (1966) also suggests that $C_b=1$ for tapered inlets. Metzler and Rouse (1959), Henderson (1966), and French (1966) all use the upstream water depth rather than the headwater specific energy in their performance equations. For choked channel contractions, Wu and Molinas (2001) use a modified form of the contraction coefficient presented by Hager and Dupraz (1985) for an infinitely wide approach channel. For an abrupt inlet, their contraction coefficient gives $C_b=0.83$. For 90° wingwall flares, the FHwA equations correspond to $C_b=0.815$ (see Table 1).

For submerged inlet conditions, Henderson (1966) presents a performance equation similar to Eq. (5). He suggests that $C_c=0.6$ for sharp-edged entrance conditions and $C_c=0.8$ for rounded soffit and vertical edges. The FHwA equations correspond to $C_c=0.754$ (see Table 1). Bos (1989) presents data showing that the contraction coefficient for a vertical sluice gate varies with the upstream headwater depth, and for $y_1/D=1.5$ (lowest value presented, where y_1=headwater depth) the contraction coefficient is $C_c=0.648$. Data for vertical sluice gates from Montes (1997) give contraction coefficients ranging from 0.65 to 0.7 for the range of headwater/culvert rise ratios of interest in this paper.

The soffit contraction coefficient, C_c, determined from the experimental data of Fig. 6(a) is consistent with the literature values cited herein. However, the vertical edge contraction coefficient, C_b, is larger than values suggested by previous investigators. One reason for this difference is likely associated with the use of multiple barrels in these experiments (only single-barrel culverts were considered by other investigators). The lack of transverse flow along the culvert headwall would reduce the vertical edge contraction effects. The value $C_b=1.0$ is considered appropriate for multiple-barrel box culverts, except possibly for culvert sides located at the ends of the culvert system, where transverse flow along the headwall can occur. Nevertheless, Fig. 6(a) shows that data from the single-barrel culvert experiments are also consistent with the proposed model.

Design Recommendations

The performance curves that were developed and fit to the experiment data from the physical model may be used to develop design equations for multiple-barrel low-headwater box culverts. These equations provide the total culvert span required for a total channel design discharge and limiting headwater.

The performance curves for box culverts are specified by Eqs. (2) and (5), with parameter values $C_b=1$ and $C_c=2/3$. These equations may be written as

$$\frac{HW}{D}=\frac{3}{2}\left(\frac{Q}{A\sqrt{gD}}\right)^{2/3} \tag{15}$$

$$\frac{HW}{D}=\frac{9}{8}\left(\frac{Q}{A\sqrt{gD}}\right)^{2}+\frac{2}{3} \tag{16}$$

According to Eq. (7), the transition between these performance curves occurs at $HW/D=1.0$. While the culvert entrance does not actually become submerged at this transition, the hydraulics of the flow changes from weir-type to sluice-type at $HW/D=1$.

For design of low-headwater highway culverts, the culvert rise D is usually determined by roadway elevation constraints, and specification that the upstream water depth under design conditions is equal to the culvert rise will allow for the thickness of the roadway and curb above the culvert soffit to act as a freeboard. As an initial assumption, one may use $y_1=D$, where y_1=headwater depth. Thus, $HW/D>1$ for design of box culverts, and Eq. (16) provides the design performance curve. If it is further assumed that $v_1=Q/(BD)$, then Eq. (16) gives

$$\frac{v_1^2/2g}{D}=\frac{4}{9}\left(\frac{HW}{D}-\frac{2}{3}\right) \tag{17}$$

With Eq. (17) one finds

$$\frac{y_1+v_1^2/2g}{D}=\frac{HW}{D}=1+\frac{4}{9}\left(\frac{HW}{D}-\frac{2}{3}\right)=\frac{4}{9}\frac{HW}{D}+\frac{19}{27}$$

This equation gives

$$\left.\frac{HW}{D}\right|_D=\frac{19}{15} \tag{18}$$

Using this value in Eq. (16) gives the design relationship

$$\left.\frac{Q}{BD\sqrt{gD}}\right|_D=\sqrt{\frac{8}{9}\left(\frac{19}{15}-\frac{2}{3}\right)}=\sqrt{\frac{8}{15}}\cong 0.73 \tag{19}$$

Eq. (19) may be used to support design calculations for highway culverts that are limited by upstream headwater depths. The usual design situation has the design discharge known, along with the maximum culvert rise that is fixed by highway design. Eq. (19) may then be used to calculate the total culvert span for the design discharge Q_T and culvert rise D

$$B|_D=\frac{Q_T}{0.73\sqrt{g}(D)^{3/2}} \tag{20}$$

In contrast, if the FHwA equations are used (as represented by $C_b=0.815$, $C_c=0.754$; see Table 1) with $HW/D=19/15$, then Eq. (5) gives $Q/[A(gD)^{0.5}]=0.62$. This results in a culvert span that is 17% larger than predicted by Eq. (20). This difference is significant, especially for multiple-barrel box culverts, where flow distribution among the culvert barrels may not be uniform and sedimentation problems can develop within outer culvert barrels.

Conclusions

The developments presented in this paper provide a simple model for description of culvert performance under both unsubmerged and submerged conditions. Application of the model equations to experimental data for multiple-barrel box culverts is also discussed. Specific conclusions include the following:

- The model presented in Eqs. (2) and (5) provides a versatile two-parameter model for describing culvert hydraulic performance for a range of culvert types and materials.
- The transition between the unsubmerged- and submerged-type flow conditions is well defined by the model and expressed in

J. Hydraul. Eng. 2006.132:474-481.

Eqs. (7) and (8). The transition between the unsubmerged- and submerged-type flows is continuous and smooth.
- For application to multiple-barrel box culverts, the contraction coefficients $C_b=1$ and $C_c=2/3$ are recommended, resulting in the performance curves given by Eqs. (15) and (16).
- For application to low-headwater highway culverts, the suggested design Eq. (20) specifies the total culvert span required for a given design channel discharge and limited culvert rise.
- For a specified channel design discharge, the resulting model gives a smaller culvert size than would be obtained using the FHwA equations.

Performance equations are generally applied for design of culverts when the upstream flow is subcritical. However, a number of the data used to fit the performance equations [Fig. 6(a)] have supercritical upstream conditions. During the experiments, supercritical flow is established through the upstream channel expansion and is not associated with a supercritical channel slope. There are concerns with the use of supercritical flow data, in that they are inconsistent with the model assumptions used to develop Eq. (2). Issues associated with supercritical flow conditions are discussed in the Appendix. The model Eqs. (15) and (16) are specifically recommended for low-headwater multiple-barrel box culverts. For low-headwater conditions, the velocity head may contribute significantly to the headwater value. The data shown in Fig. 6(a) includes a wide range in depth and velocity head contributions to specific energy. The model presented in Eqs. (2) and (5) is capable of representing culvert performance over a wide range of hydraulic conditions.

Acknowledgments

Research support from the Texas Department of Transportation is greatly appreciated. The writers especially wish to acknowledge the interest and support received from George (Rudy) Hermann, who served as Project Director during this research effort.

Appendix

For culvert design conditions, it has generally been assumed that the upstream flow is subcritical and that headwater depth and specific energy may be used interchangeably. However, for some of the data from the laboratory experiments, the velocity head is a significant part of the specific energy, and the upstream flow is supercritical. Fig. 7 shows a normalized plot of the measured depth versus specific energy upstream of culvert barrels for all of the data in Fig. 6(a). If all of the data lay near the 1-to-1 line, then culvert performance could be predicted by upstream depth. The expression for the headwater may be written as

$$\frac{HW}{D}=\frac{E}{D}=\frac{y}{D}+\frac{v^2}{2gD}=\frac{y}{D}\left(1+\frac{F^2}{2}\right) \tag{21}$$

Using Eq. (21), lines are drawn on Fig. 7 marking the relationship between depth and specific energy for Froude number (F) values of 1 and 2 (a Froude number value of 0 corresponds to the 1-to-1 line). A number of data for the four- and six-barrel culvert systems fall between the $F=1$ and $F=2$ lines, showing that for these experiments the approach flow is supercritical. The flow becomes supercritical as it passes through the channel expansion upstream of the culvert system; the channel slope is small.

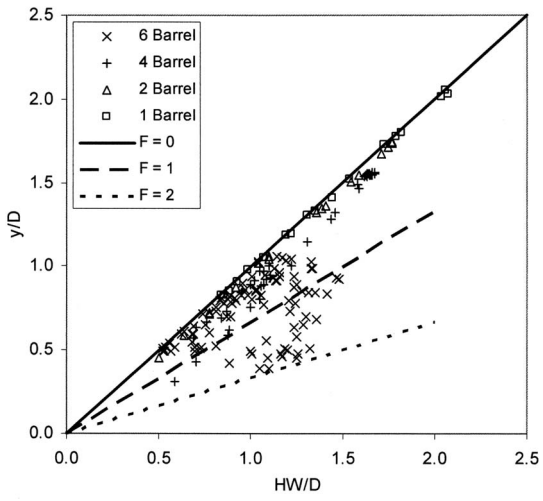

Fig. 7. Performance data [all data from Fig. 5(a)] showing depth versus specific energy. Lines corresponding to Froude numbers $F=1$ and $F=2$ are shown.

There is some question as to use of the performance equations for upstream supercritical flow conditions. The reason for this concern is that, while subcritical flow will adjust upstream to conform to the culvert inlet acting as a control (backwater effects), supercritical flow cannot adjust to establish critical flow conditions within the culvert inlet, which is the basis of Eqs. (1) and (2). An arbitrary set of data with a large Froude number was examined to evaluate consistency with the model assumptions. The depth and velocity were measured 0.6 m upstream of the culvert entrance for the six-barrel culvert box with all barrels open. The channel discharge was 0.244 m^3/s. As was usual, the distribution of specific energy was not uniform across the culvert barrels, so the discharge through each barrel was not the same. The headwater in barrels 2, 3, and 5 suggested that they had approximately the same discharge, and measured data for these barrels are compared in Fig. 8 (the estimate barrel discharge values are 0.0495, 0.0489, and 0.0502 m^3/s, respectively). The Froude number lines corresponding to $F=0$, 1, and 2 are shown in Fig. 8, as are the specific energy curves for the headwater and

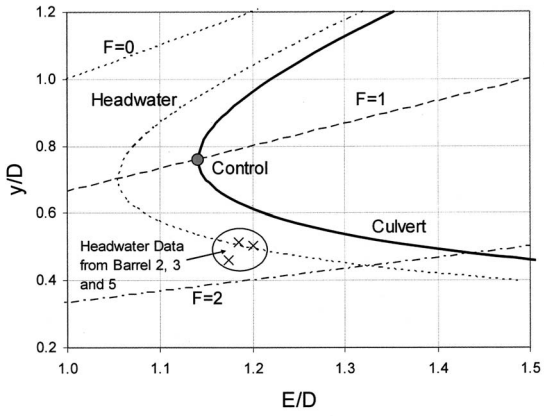

Fig. 8. Headwater data from three culvert barrels for data set ($Q_{barrel}\sim 0.049$ m^3/s) with supercritical flow upstream of culvert entrance. Headwater and culvert entrance specific energy curves are shown, as are lines corresponding to $F=0$, 1, and 2.

J. Hydraul. Eng. 2006.132:474-481.

culvert entrance. These curves differ because of flow contraction going into the culvert. The model culvert box used customary U.S. "2×8" lumber for the culvert side walls, which measures 0.038 m in thickness and 0.184 m in height. The thickness of one side wall (half for each side of the barrel) is added to the barrel width to give the upstream flow width, which contracts to a culvert box width of 0.305 m upon entering the culvert. Fig. 8 also shows the culvert control point that corresponds to the intersection of the F=1 line and the culvert specific energy curve. Data for the three barrels are consistent with headwater depth and specific energy. A transition to control upon entering the culvert would require a small head loss. Otherwise, it is likely that the depth increases but the flow remains supercritical upon entering the culvert box. Other data with lower Froude number values (but still supercritical) are also found to be consistent with a transition from supercritical flow upstream to critical flow within the culvert barrel. For all of the data, both subcritical and supercritical, the measured specific energy distribution and barrel discharge are consistent with the performance Eqs. (15) and (16).

Notation

The following symbols are used in this paper:

A = box culvert full cross-section area;
B = box culvert span;
C_b = culvert width contraction coefficient;
C_c = culvert soffit contraction coefficient;
c = FHwA equation constant (dimensional) for submerged entrance;
D = box culvert rise;
E_c = critical specific energy;
g = gravitational constant;
HW = headwater specific energy;
K = FHwA equation constant (dimensional) for unsubmerged entrance;
M = FHwA equation constant for unsubmerged entrance;
N = number of data;
Q = discharge;
Q_{barrel} = barrel discharge;
Q_i = corrected barrel discharge;
Q_i^* = calculated barrel discharge;
Q_T = total channel discharge;
S = culvert barrel slope;
v_{en} = velocity within culvert entrance;
v_1 = headwater (approach) velocity;
Y = FHwA equation constant for submerged entrance;
y = depth;
y_c = critical depth; and
y_1 = headwater (approach) depth.

References

American Society of Civil Engineers/Water Environment Federation (ASCE). (1992). *Design and construction of urban stormwater management systems*, ASCE, New York.

Bos, M. G. (1989). *Discharge measurement structures*, 3rd Ed., International Institute for Land Reclamation and Improvement, Wageningen, The Netherlands.

Brunner, G. W. (2002). *HEC-RAS river analysis system hydraulics reference manual*, U.S. Army Corps of Engineers, Hydrologic Engineering Center, Davis, Calif.

Charbeneau, R. J., Henderson, A. D., Murdock, R. C., and Sherman, L. C. (2002). "Hydraulics of channel expansions leading to low-head culverts." *Research Rep. 2109-1*, Center for Transportation Research, Univ. of Texas at Austin, Austin, Tex.

Chow, V. T. (1959). *Open-channel hydraulics*, McGraw-Hill, New York.

Clemmens, A. J., Strelkoff, T. S., and Replogle, J. A. (2003). "Calibration of submerged radial gates." *J. Hydraul. Eng.*, 129(9), 680–687.

French, J. L. (1955). "First progress report on hydraulics of culverts: Hydraulic characteristics of commonly used pipe entrances." *NBS Rep. 4444*, National Bureau of Standards, Washington, D.C.

French, J. L. (1966). "Fifth progress report on hydraulics of culverts: Nonenlarged box culvert inlets." *NBS Rep. 9327*, National Bureau of Standards, Washington, D.C.

Hager, W. H., and Dupraz, P. A. (1985). "Discharge characteristics of local, discontinuous contractions." *J. Hydraul. Res.*, 23(5), 421–433.

Henderson, F. M. (1966). *Open channel flow*, Macmillan, New York.

Herr, L. A., and Bossy, H. G. (1965). "Hydraulic charts for the selection of highway culverts." *Hydraulic Engineering Circular No. 5 (HEC-5)*, Federal Highway Administration, Washington, D.C.

Mavis, F. T. (1943). "The hydraulics of culverts." *Bulletin No. 56*, Pennsylvania State Univ., State College, Pa.

Metzler, D. E., and Rouse, H. (1959). "Hydraulics of box culverts." *Bulletin 38*, Iowa State Univ., Ames, Iowa.

Montes, J. S. (1997). "Irrotational flow and real fluid effects under planar sluice gates." *J. Hydraul. Eng.*, 123(3), 219–232.

Normann, J. M., Houghtalen, R. J., and Johnson, W. J. (1985). "Hydraulic design of highway culverts." *Hydraulic Design Series No. 5*, 2nd Ed., Federal Highway Administration, Washington, D.C.

Sturm, T. W. (2001). *Open channel hydraulics*, McGraw-Hill, New York.

Wu, B., and Molinas, A. (2001). "Choked flows through short contractions." *J. Hydraul. Eng.*, 127(8), 657–662.

Yarnell, D. L., Nagler, F. A., and Woodward, S. M. (1926). "Flow of water through culverts." *Bulletin 1*, Iowa State Univ., Ames, Iowa.

J. Hydraul. Eng. 2006.132:474-481.